ASTRONOMY & ASTROPHYSICS
SUPPLEMENT SERIES

Astron. Astrophys. Suppl. Ser. **118,** 65-87 (1996)

Galaxy population in distant galaxy clusters. I. Cl 0939+472 (z=0.41) and Cl 0016+161 (z=0.54)

P. Belloni[1,2] and H.-J. Röser[1]

[1] Max-Planck Institut fur Astronomie, Königstuhl 17, 69117 Heidelberg, Germany
[2] Institut für Astronomie und Astrophysik, Scheinerstraße 1,81689 München, Germany
email: belloni@usm.uni-muenchen.de

Received March 13; accepted December 14, 1995

Abstract. — ⋆ We present results of a study of the galaxy population of Cl 0939+472 ($z = 0.41$) and Cl $0016 + 161$ ($z = 0.54$). We have used narrow-band filters (FWHM $\simeq$ 90 – 200 Å) and broad band B, R, I filters covering the range from 3800 Å to 9200 Å to obtain low resolution spectra for all galaxies brighter than $R = 22.5$ mag in a $5' \times 5'$ (Cl $0939 + 472$) and a $3.5' \times 5'$ (Cl $0016 + 161$) field. Template spectra for classical Hubble type and E + A galaxies were fitted to the low-resolution spectral energy distribution in order to determine the galaxies' redshift and the morphological type. We detected 160 cluster members in Cl $0939 + 472$ and 100 in Cl $0016 + 161$, with a success rate of about 80% in the determination of redshifts and corresponding classification of morphological types from spectral energy distributions. These results constitute a statistical improvement of at least a factor of 4 over the most complete study to date of these clusters. In particular, we provide a large sample of elliptical galaxies with secure membership, well suited for a study of evolutionary effects. The same E + A templates developed for the analysis of Cl $0939 + 472$ were successful in recognizing almost all of the spectroscopically already known E + A galaxies in Cl $0016 + 161$ and in identifying 10 new ones. Our results show that in this cluster, too, the fraction of E + A galaxies represents about 20% of the total galaxy population. This outlines the importance of taking into account galaxies with signs of recent star formation for a correct evaluation of the Butcher-Oemler effect in distant galaxy clusters.

Key words: galaxies: clusters: Cl $0939 + 472$; Cl $0016 + 161$ — galaxies: clusters; redshifts; evolution

1. Introduction

The interest in studying the galaxy population of high redshift galaxy clusters comes from the discovery of the Butcher-Oemler effect (Butcher & Oemler 1978), namely that high redshift ($z \geq 0.2$) rich clusters show a significantly higher population of blue galaxies compared to their lower redshift counterparts. The Butcher-Oemler effect was initially faced with a lot of skepticism because galaxy membership cannot be determined from photometry alone and statistical corrections are needed to remove the contamination from field galaxies. However, a series of following photometric and spectroscopic work (Dressler & Gunn 1983; Lavery & Henry 1986 1987; Dressler & Gunn 1992 (hereafter DG92); Couch & Sharples 1987) have meanwhile confirmed this evolutionary effect. In addition to blue cluster members showing signs of ongoing star formation, spectroscopy also revealed galaxies (now called E+A) with a spectrum typical for ellipticals but with overlying strong Balmer absorption lines ($\overline{\mathrm{EW}}(\mathrm{H}_\beta+\mathrm{H}_\gamma+\mathrm{H}_\delta) \geq 7-8$ Å), evidence for them to have recently concluded an episode of star formation (Dressler et al. 1983). These galaxies span a wide range in colors, being often only 0.2 magnitudes bluer in $B - V$ than cluster ellipticals and therefore they will not easily show up as unusual in photometric studies. While E+A galaxies are very rare in rich, nearby galaxy clusters (Dressler 1980) their fraction in cluster at $z = 0.4 - 0.5$ can reach 20% (Dressler & Gunn 1992). Therefore, to avoid underestimating the real fraction of galaxies with signs of ongoing or recent star formation activity, the Butcher-Oemler effect is nowadays more appropriately formulated in terms of the passive-to-active galaxy ratio rather than the blue-to-red ratio.

Despite the progress made in multi-slit spectroscopy up to date only a handful of rich clusters have been studied in a systematic way, i.e. conclusions about the amount of galaxy evolution have not been obtained with statistically significant und unbiased samples of cluster members. Recently, the Hubble Space Telescope (HST) has allowed

Send offprint requests to: P. Belloni
⋆Tables 4 and 5 are also available in electronic form at the CDS via anonymous ftp 130.79.128.5

us to distinguish morphology of distant galaxies and thus probe directly the processes driving galaxy evolution. HST images confirm the connection of disturbed morphology with starburst or emission line galaxies, but the majority of the blue galaxies look like normal disk systems (Couch et al. 1994; Dressler et al. 1994). Also E+A galaxies show different morphologies. Indeed, in AC114 (Couch et al. 1994) most of them appear to be unremarkable, bulge-dominated systems, whereas those in Cl 0016+161 (Wirth et al. 1994) and Cl 0939 + 47 (Dressler et al. 1994; Belloni et al. 1995) are consistent with a disk-like appearance or interacting/merger systems. This suggests that interactions between galaxies play a role in triggering star formation but it is more likely that non-disruptive interactions among galaxies (Moore et al. 1996) or/and galaxies and the intra-cluster medium are the dominant mechanisms (Bothun & Dressler 1986).

Despite the importance of the morphological information, it must however be stressed that HST images do not provide the galaxies' membership, without which only statistically considerations can be done.

Bearing in mind the importance of a secure cluster membership for any conclusion regarding galaxy evolution we began a project to develop tools to analyse the galaxy populations in high redshift clusters more reliably and efficiently than previously done. The primary goals have been: use photometric imaging methods, establish a large number of galaxies as cluster members and classify each member galaxy according to its type. The approach followed is twofold; a Fabry-Perot Interferometer is used to search for redshifted [OII]λ3727 line emission from galaxies with ongoing star formation (Thimm et al. 1994) whereas an appropriate combination of broad and narrow band filters detect features typical of elliptical and E+A galaxies (Belloni et al. 1995).

In Belloni et al. (1995) we extensively described the advantages of multifilter photometry applied to the study of Cl 0939 + 472. The use of narrow bandpasses rather than direct spectroscopy produces some loss in spectral resolution but gains in increased signal-to-noise per object and coverage of the entire cluster per exposure. A remarkable result of this procedure was the success in identifying E+A galaxies that turned out to be a significant fraction (≈20%) of the cluster population.

In the present paper we report the results obtained by means of optimized multi-filter photometry for the whole cluster population in Cl 0939 + 472 and Cl 0016 + 161. Cl 0016 + 161 has historically received much attention, because it is optically very rich (Koo 1981) and lies at a relatively high redshift ($z = 0.54$). In confirmation of this richness, it is one of the brightest X-ray clusters known (Henry et al. 1992). Photometrically, its galaxy population is dominated by red galaxies (Koo 1981; Ellis et al. 1985; Aragon-Salamanca et al. 1993) but spectroscopic evidence of recent star formation in many of the red galaxies (DG92) puts the fraction of active galaxies in Cl 0016+161 among the highest known.

The analysis of Cl 0016 + 161 has been performed following the same approach as in Cl 0939 + 472. Therefore, paragraphs on observations, reduction of the photometric and spectroscopic data and determination of the galaxy redshift and morphological type, will outline only aspects peculiar to the study of Cl 0016 + 161. The discussion of the results presented here and a comparison of the galaxy populations of four distant clusters will be the subject of a forthcoming paper.

Table 1. Log of photometric observations. (1) Mean wavelength of filter passband/FWHM. (2) Rest frame wavelength. (3) Date (4) Total exposure time/number of exposures. The exposure time required for a complete analysis of cluster is also shown (in hours). (5) Seeing (6) Broad band filters and those that define the $\tilde{D}_{4000}$

[Å] (1)	[Å] (2)	(3)	[s]/num. (4)	[″] (5)	(6)
4400/1150	2850	20.11.92	5000/5	≤ 1.0	B
4930/540	3200	8.11.91	2000/4	1.2	
5770/120	3740	22.11.92	6000/4	1.0	
6040/210	3920	9.11.91	3000/6	1.2	$\tilde{D}^{-}_{4000}$
6240/120	4050	9.11.91	3000/3	1.2	
6330/110	4110	10.11.91	4000/4	2.0	$\tilde{D}^{+}_{4000}$
6650/180	4320	11.11.91	3000/4	1.2	
6550/1690	4250	20.11.92	900/3	1.0	R
7250/150	4700	10/11.11.91	4500/5	2.0–1.2	
8020/120	5200	25/26.11.92	5000/5	1.0	
8200/1300	5810	20.11.92	600/2	≤ 1.0	I
			$\Sigma \simeq 11$ h		

2. Observations

Cl 0016 + 161 was observed at the prime focus of the 3.5 m telescope on Calar Alto (Spain) in November 1991 and November 1992. We used a 1024^2 Tektronix CCD (pixel size 25 μm and 8 e^- readout noise) with a scale of 0.53″/pix and a field of view of $7' \times 7'$. The log of observations of Cl 0016+161 is shown in Table 1 and the effective transmission for each filter/detector combination in Fig. 1. The filters were selected to detect features characteristic of the spectral energy distributions (SED) of ellipticals and E+A galaxies at the cluster redshift. In particular, two of the narrow-band filters have been chosen to reproduce as accurately as possible the 4000 Å-break index (D_{4000}) defined spectroscopically by Bruzual (1983). The photometric definition adopted here for Cl 0016 + 161 is $\tilde{D}_{4000} = 1.162 \times F_\lambda(6330/110)/F_\lambda(6040/210)$. The $\tilde{D}_{4000}$ notation emphasizes that we are not dealing with the standard index. It is worth mentioning that our photometric

approach allows us to measure $\tilde{D}_{4000}$ for hundreds of cluster galaxies at once.

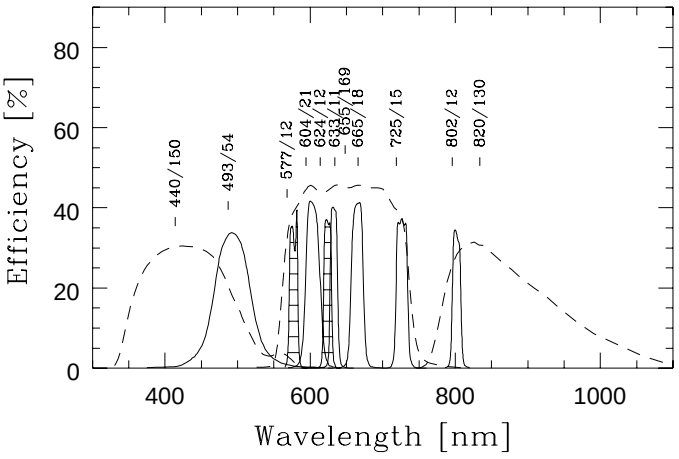

Fig. 1. Total efficiency of the filter+detector system used to sample the the spectral energy distributions of the cluster galaxies. The filters that define the 4000 Å-break are shaded

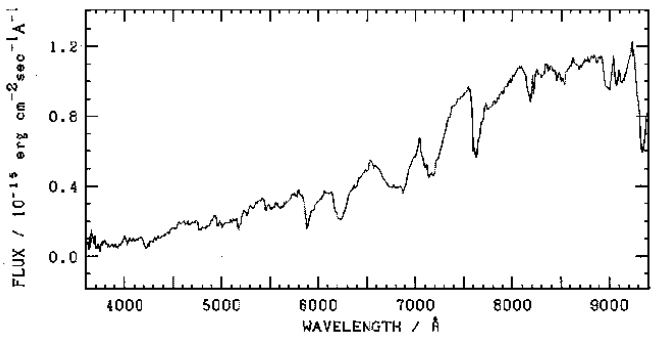

Fig. 2. Spectrum of the star in the field of Cl 0016 + 161 used to calibrate the filter data. Its spectral type is M4V

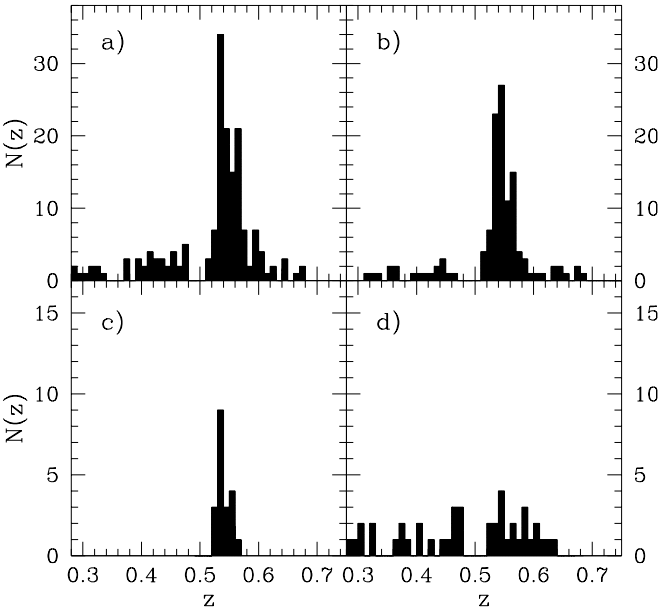

Fig. 3. Redshift distribution in Cl 0016 + 161 of **a)** all objects classified, **b)** all elliptical, **c)** all E+A and **d)** all spiral/Im galaxies

3. Data reduction

For the bias, flat field, cosmic rays and fringe corrections, the procedure described in Röser & Meisenheimer (1991) was followed. We recall only that the flat field correction was performed by taking, for every filter, several offset exposures of the twilight sky. When this procedure did not succeed in flattening the science frames' background to better than 1%, the science frames themselves were used to produce a model of the background. For the I filter, the only one that showed residual fringes, a fringe frame was derived from the science flat field and treated as an additive flat field component.

To extract from the Cl 0016 + 161 field a statistically complete sample of objects the INVENTORY package implemented in MIDAS was used. Our Cl 0016 + 161 sample (380 objects) was defined by extracting all objects brighter than $R = 23.5$ above an isophotal level of 26 mag/$\Box''$ in a $3.5' \times 5.5'$ field, corresponding to the somewhat elongated appearance of the cluster.

Because the cluster field is very crowded, we did not use a simple fixed aperture photometry to extract fluxes. Instead, we applied a weighted summation procedure (Röser & Meisenheimer 1991). The width of the weighting function was chosen in such a way to produce an effective resolution of all measurements of 2.2″ FWHM, set by the image with the worst seeing (Table. 1). This ensures that frames taken in different photometric conditions could be properly added.

3.1. *Spectrophotometry*

The relative flux calibration of the filter data was performed by taking the spectrum of a star in the cluster field ($\alpha = 00^{\rm h}\ 15^{\rm m}\ 59^{\rm s}$, δ=16°02′30″ (1950), Fig. 2). The spectroscopic setup employed is the same as described in Belloni et al. (1995). Combining this calibration spectrum with the filter/detector system efficiency curves for every frame, we obtained the count-to-flux conversion factors. The main advantage of this procedure, with respect to the calibration using spectrophotometric standard stars, is that the cluster calibration is then unaffected by variations of the photometric conditions during the night and

Fig. 4. Redshift derived from our filter data compared with values obtained by Dressler & Gunn (1992). The dashed line represents the expected locus of the data points in the case of perfect agreement. The error bars indicate the 1σ-error of the redshift. The σ_z is 0.012

even frames taken in different observing runs can be easily combined. For the flux calibration of the target star the standard stars Feige 110 and BD $2626+06$ were used (Massey et al. 1990). No interstellar correction was applied because in the direction of Cl $0016+161$ the $E(B-V)$ is ≤ 0.03 (Burstein & Heiles 1982).

4. Results

4.1. *Redshift and galaxy type*

Cluster membership and spectro-morphological class of the galaxies have been determined by fitting the observed fluxes (low-resolution SEDs) with template spectra of local galaxy types. The templates comprise the type E, Sbc, Scd and Im taken from Coleman et al. (1980) and the model spectra for E+A galaxies developed in Belloni et al. (1995) with Bruzual & Charlot (1993) population synthesis models. E+A templates have been generated under the assumption that these galaxies result from a strong burst of star formation occurring in an early-type galaxy. The eight SEDs represent the temporal evolution of the elliptical+burst SED where the burst last 0.25 Gyr and contributes 20% of the total mass of the galaxy. The spectral evolution of this composite model is followed up to 2.5 Gyr after the burst completion. Older bursts, indeed, cannot be distinguished from normal, passively evolving ellipticals without more accurate spectral indices that require high signal-to-noise spectra (Pickles 1985; Rose 1985).

Finally, all templates have been redshifted stepwise by Δz=0.002 in order to cover the redshift interval between $z = 0.3$ and $z = 0.7$ and convolved with the filters/detector setup.

Some aspects of this procedure are worth mentioning. First, the selection criterion applied to define the sample of elliptical galaxies. Our classification of a galaxy as an elliptical relies on its match over a large wavelength range (rest frame $2800-5500$ Å) to the SED of a nearby elliptical. Therefore, our elliptical sample fulfills a much more restrictive condition than a sample defined by means of a two or three colors criterion. Consequently, we can reliably bring into view evolutionary effects in elliptical galaxies, either those expected from the passive scenario and more flamboyant one, e.g. abnormally powerful secondary star formation events.

Second, the cutoff of our galaxy sample has been set 3 magnitudes fainter than present-day L^*, the characteristic break on the luminosity function. We thus cover a significant tail of the cluster population and do not select just the bright elliptical members in which evolutionary effects are known to be minimal (Aragon-Salamanca et al. 1993; Dickinson 1995). Third, by using non evolved SEDs we have assumed that the correspondence between spectral type and morphological type is still valid at the clusters' look-back times. The assumption that evolutionary effects are at first order negligible is well confirmed by the results in Table 8 of Belloni et al. (1995). There is shown that in Cl $0939+472$ morphological information derived from optimized narrow band photometry is substantially in agreement with that provided by HST imaging observations (Dressler et al. 1994), confirming the efficiency of this approach in the recognition of morphological types of distant galaxies.

The results of the analysis for Cl $0016+161$ are presented in Table 2. Notice that out of the 200 objects, 161 could be classified, representing a success rate of 80% in the determination of redshifts and corresponding morphological types from SEDs. 39 objects have been considered non-classifiable because they could not be reliably fitted with any of the SED templates at any redshift, i.d. a minimum $\chi^2$of the predicted to the observed fluxes gave a $\sigma_z \geq 0.06$.

In Fig. 3a we report the resulting redshift distribution for all classified objects in the redshift range analyzed ($0.30 < z < 0.70$) whereas in Figs. 3b-d they are further separated by morphological type. The existence of a cluster in the field is clearly shown by a peak in correspondence of the cluster redshift, whereas a significant wing is visible at $z = 0.60-0.65$ and a possible foreground component at $z = 0.30-0.40$. Ellis et al. (1985) already suggested that the visual richness of Cl 0016+161 could be partially due to the the existence of a foreground cluster. Although with our more comprehensive sample the number of galaxies with $z = 0.30-0.40$ has increased to 19, we believe that they more likely represent field galaxies than a foreground cluster. Indeed their spatial distribution is not clumped. They look instead as a loose structure filling the whole $3.5' \times 5'$ area.

Clearly, the accuracy with which we can estimate redshifts for non cluster galaxies is lower than that for cluster members to which the filter setup has been optimized.

Table 2. Results of the redshift analysis of the Cl 0016 + 161 field. All objects with $m_R \leq 22.5$ have been considered

Tot Obj.	Memb.	Backgr.	Foregr.	Stars	Not Ident.	Compl.
200	101	17	31	12	39	80%

Table 3. Galaxy population in Cl 0016+161. The mean values for colors and $\tilde{D}_{4000}$ are indicated. A color-magnitude correction has been applied to the elliptical galaxies

Spectral type	DG92	This work	$< B-R >$	$< B-I >$	$< \tilde{D}_{4000} >$
Elliptical	19	73	2.82±0.21	4.30±0.24	2.10±0.45
E+A	10	20	2.11±0.34	3.17±0.45	1.74±0.23
Spiral & Im	2	7	1.69±0.34	2.75±0.34	1.18±0.22

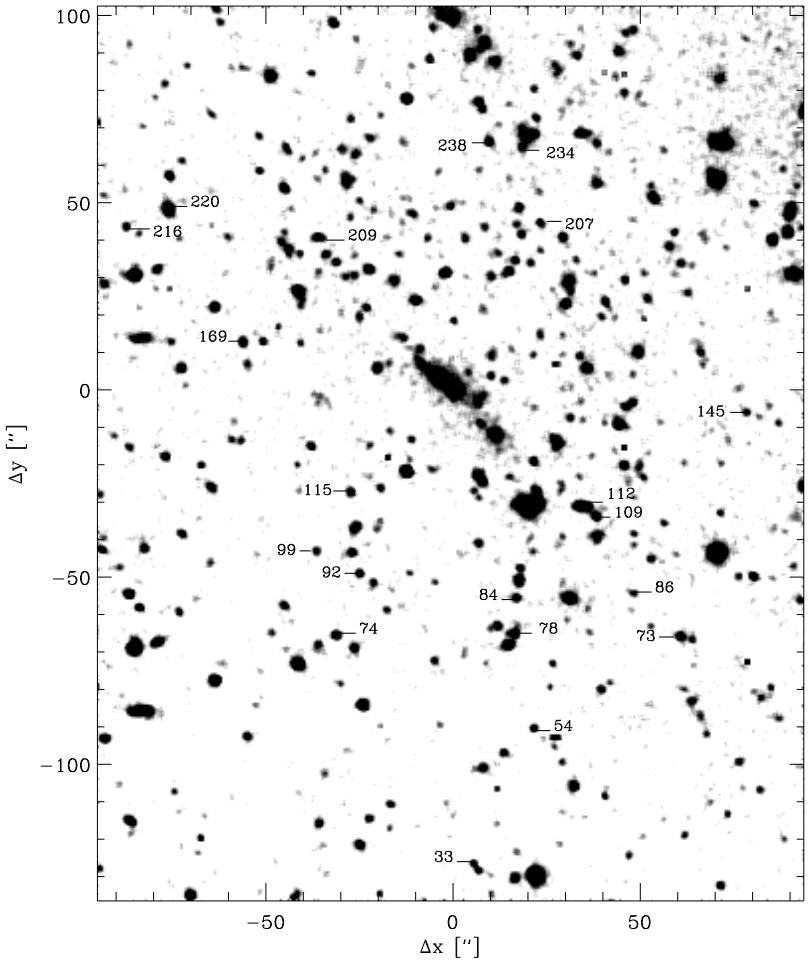

Fig. 5. Red image of a $3.5' \times 5'$ field in Cl 0016 + 161. E+A galaxies are labelled

However, five foreground and five background galaxies with redshifts published by DG92 have been correctly identified.

Concerning the accuracy achieved in the determination of the redshift for the elliptical and E+A population, we plot in Fig. 4 the redshifts of 17 elliptical galaxies which are spectroscopically confirmed as members (DG92) versus those obtained here using narrow band filters. The standard deviation σ_z(narrow band−spectroscopy)=0.015 and the mean cluster redshift obtained with the whole elliptical sample is $z = 0.552 \pm 0.015$, in agreement with the DG92 value of $z = 0.5455$.

As a criterion to define the cluster membership for elliptical and E+A galaxies we considered a $\pm$ 3 σ_v in the cluster rest frame taking the cluster velocity dispersion spectroscopically determined by DG92, i.e. $\sigma_v \simeq$1300 km s^{-1}. Consequently, all ellipticals and E+A galaxies with redshift in the range $0.530 < z < 0.570$ have been considered cluster members.

For spiral and irregular galaxies we could not provide a comparable accurate membership and indeed a detailed study of this cluster population is beyond the scope of this work. Figure 3d shows that the broad distribution of spiral/irregular cluster members around the mean redshift cannot be clearly disentangled from the background component at $z = 0.60 - 0.65$. Furthermore, a comparison of the redshift obtained for the two spectroscopically known emission line galaxies (#213 and #239) shows that a Δz(narrow band–spectroscopy)=0.04 is well possible. Aware of these uncertainties, we considered cluster members all spiral and irregular galaxies with redshift $0.52 < z < 0.58$.

Concerning the analysis of the E+A galaxies, first of all we checked that the E+A templates developed in Belloni et al. (1995) could systematically identify these galaxies in Cl 0016+161, too. This check was necessary because there is no reason a priori to assume that the same E+A templates could be adequate for all galaxy clusters; in particular that E+A galaxies in Cl 0016+161, a higher redshift and very red cluster, would have the same characteristics of those in Cl 0939 + 472. We could correctly identify all but two of the spectroscopically known E+A galaxies in Cl 0016 + 161 (DG92), and we discovered 10 new ones. The failure in classifing the galaxies #69 and #82 (respectively #106 and #134 in DG92) as E+A is probably due to their peculiar SED. Indeed, the spectrum of the galaxy 134 published by DG92 shows an unusual red continuum for such strong Balmer absorption lines and such an SED is not included in the sequence of E+A templates used. Taking into account these two galaxies too, the fraction of E+As in Cl 0016 + 161 represents 21±4% of the total galaxy population. Their spatial distribution shown in Fig. 5 strikingly indicates that E+A galaxies systematically avoid the cluster center. This confirm the results obtained for Cl 0939 + 472 and a trend generally noticed

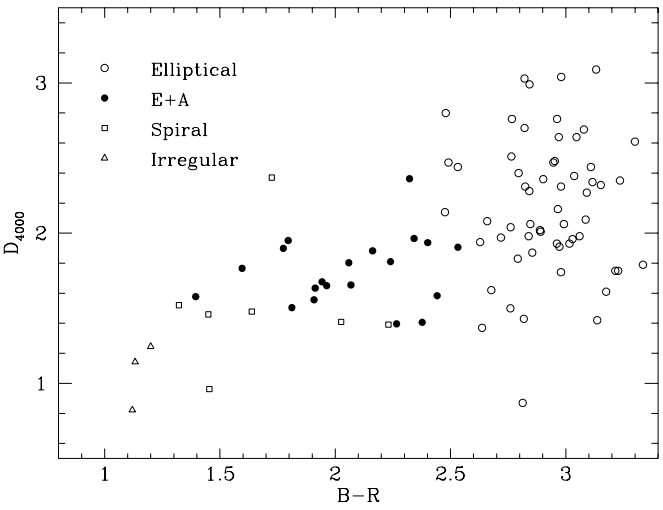

Fig. 6. Diagram showing the $\tilde{D}_{4000}$ index as a function of the $B - R$ color for the Cl 0016 + 161 members. The colors of the elliptical galaxies have been corrected for color-magnitude effect. The error bars of the photometry are also indicated

by many workers in the field (Pickles & Van der Kruit 1991; DG92). Once again the importance of our result is the statistically more significant sample which our conclusions are based on.

The diagram in Fig. 6 displays the results for all Cl 0016 + 161 members, in terms of $\tilde{D}_{4000}$ versus $B - R$ color. Color–magnitude correction (Visvanathan & Sandage 1977; Bower et al. 1992) has been applied to the elliptical galaxies. Indeed, colors and magnitudes of elliptical galaxies define a mean color-magnitude relation, according to which the colors get redder at decreasing absolute magnitude and hence increasing mass of galaxies. The validity of this relation has been observed by Aragon-Salamanca et al. (1993) and Dickinson (1995) up to redshifts of 1 and interpreted as evidence of a common, synchronized star formation history for elliptical galaxies.

Nevertheless, the first impression one receives from Fig. 6 is the large scattering in the data points for elliptical galaxies. One should however be aware that the scattering in the $\tilde{D}_{4000}$ index is partially due to its photometric definition that does not take into account the cluster velocity dispersion. Indeed, the filters were chosen to reproduce the $\tilde{D}_{4000}$ index as accurately as possible only for galaxies at the mean cluster redshift. But a σ_v=1300 km s^{-1} results in a $\Delta\tilde{D}_{4000} \simeq 0.2$ introducing then a significant broadening in the $\tilde{D}_{4000}$ values. An appropriate correction for this effect will be applied when we will discuss evolutionary effects. Nevertheless, compared to Cl 0939 + 472 (Fig. 12 in Belloni et al. 1995) for which the same procedure was used, Cl 0016+161 shows a bigger dispersion in the $\tilde{D}_{4000}$ index. A lower photometric accuracy resulting

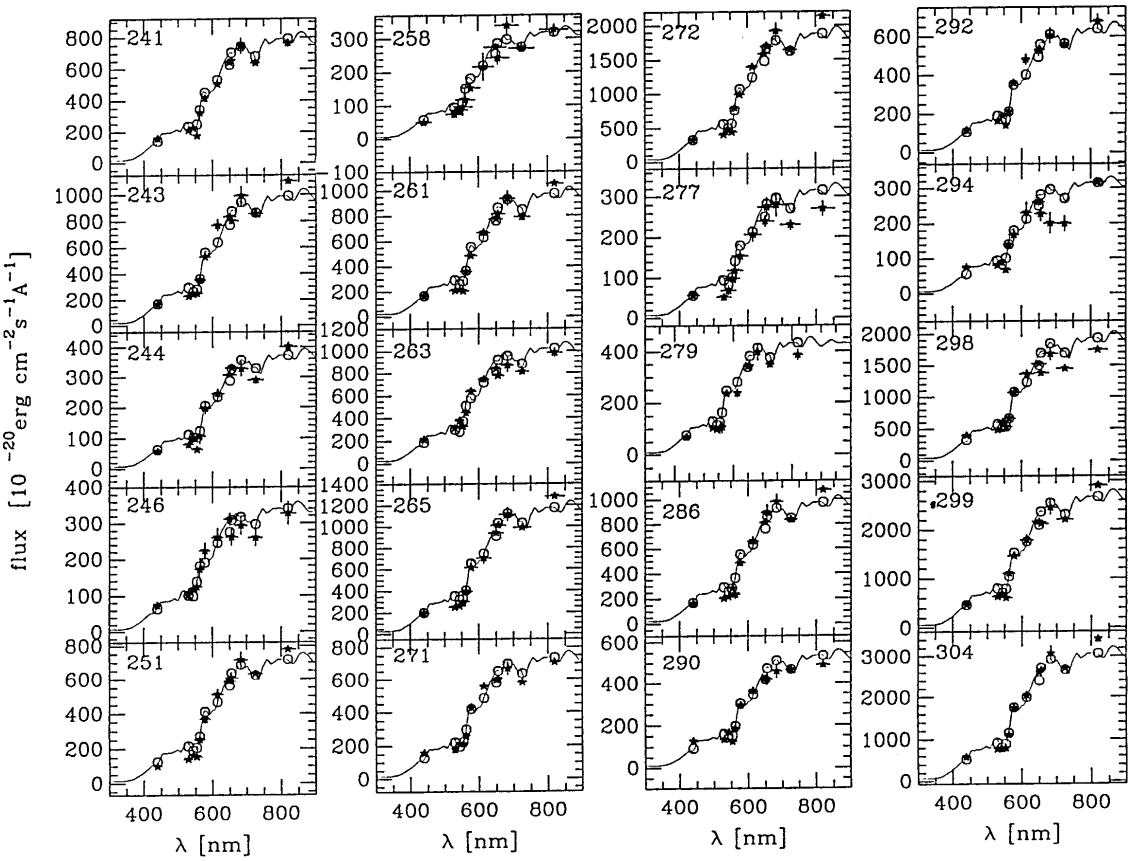

Fig. 7. Examples of low-resolution spectra of elliptical galaxies in Cl 0939+472. The empty circles represent the values expected by convolving the theoretical spectral distribution with the filters used. The filled points are the observed values. The error bars show the 1σ of the photometry. The galaxies 263, 272, 299 and 304 are already known to be cluster members from Dressler & Gunn (1992)

from the worse quality of the data (see the poor seeing of the 6330/110 filter in Table 1) could be an explanation, although a bigger intrinsic dispersion in the properties of the elliptical galaxies of this cluster cannot be ruled out. Note however that the E+A's location in this diagram is well defined because these galaxies have significantly bluer colors and lower $\tilde{D}_{4000}$ than the ellipticals.

In Table 3 we report the classification of the Cl 0016+161 member galaxies derived from their SEDs. The improvement achieved in the statistics compared with the more complete work available to date (DG92) is about a factor of 4. The number of elliptical galaxies is enhanced by a factor of 3.8, compared with a factor of 2.4 for active galaxies.

To show the good quality of the fits with which the previous results have been obtained we present in Figs. 7 and 9 examples of reconstructed low-resolution spectra of elliptical galaxies for both clusters. The 20 galaxies we classified as E+A are instead plotted in Fig. 10. In the approach we adopted, the observed differences among the E+A SEDs are attributed to the spread in age after a burst of star formation, characterized by a given duration and strength. Note the much stronger Balmer absorption lines and blue continuum in the galaxies #216 and #169 seen 0.50 and 0.64 Gyr after the beginning of the burst compared to the galaxy #220 where the burst is already 1.9 Gyr old. The histogram in Fig. 11. displays the age distribution of the 20 E+A cluster members. Although they have a rather broad distribution, young types seem to be more frequent in this cluster than in Cl 0939 + 472 (Belloni et al. 1995). It is worth recalling that an accurate assessment of the duration of the starburst and of the time elapsed since its termination requires a detailed analysis of metal and Balmer absorption lines, possible only with high resolution spectra (Rose 1985). This is, however, beyond the scope of our work. We focus indeed on developing appropriate E+A SEDs to systematically and reliably recognize this peculiar component of the cluster galaxy population. In this respect the spectra of 7 of our new elliptical and E+A cluster candidates taken with the

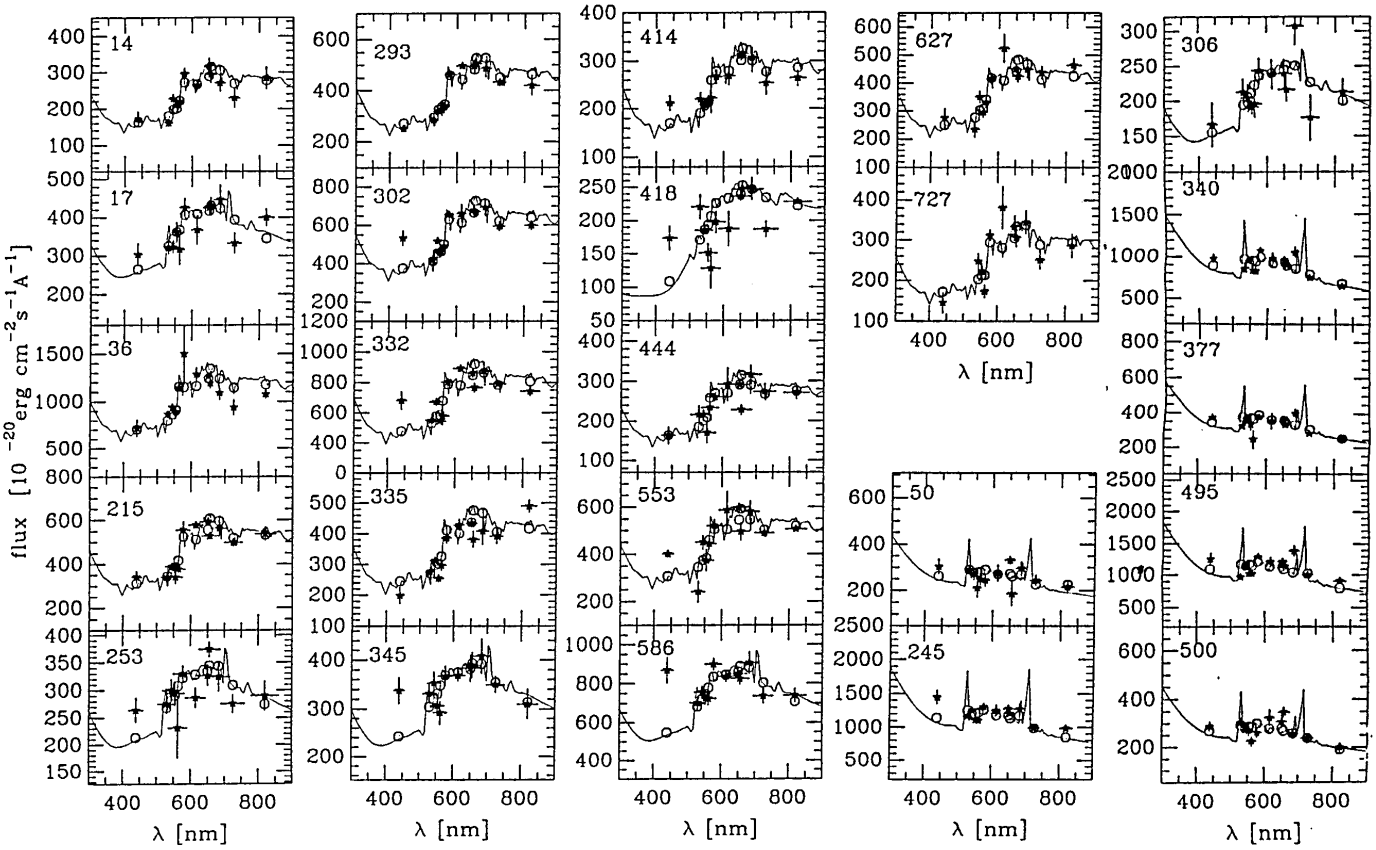

Fig. 8. Low-resolution spectra of all galaxies classified as spiral or irregular in Cl 0939 + 472. The galaxies 340 and 495 are the only already known emission line cluster members (Dressler & Gunn 1992). Same symbols as in Fig. 7

Keck telescope are very encouraging. All turned out to be cluster members and their spectral type was correctly classified (Wirth & Belloni 1996).

Though the membership of galaxies with ongoing star formation has been determined with a lower accuracy, we show in Figs. 8 and 12 the resulting fits for all galaxies classified as spiral or irregular members. This gives a qualitative idea of the accuracy of our classification. Besides the very few spectroscopically known members (#340 and #495 in Cl 0939 + 472 and #213 and #239 in Cl 0016 + 161), other galaxies, especially in Cl 0939 + 472, appear to have an equally well fitted SED. Therefore this multi-filter approach has, among other things, allowed us to identify a significant sample of spiral and irregular galaxies as candidate cluster members. This represents a big advantage for the necessary follow-up spectroscopy because it will deal with a reasonable number of target galaxies selected with a criterion more reliable than just their blue colors.

Finally, the results of the analysis of the 200 objects in Cl 0016 + 161 and 323 in Cl 0939 + 472 brighter than $R = 22.50$ are summarized in Tables 4 and 5. Coordinates, redshift, colors, $\tilde{D}_{4000}$, and morphological type are indicated. Question marks denote objects that could not be fitted by any of the templates at any redshift between $z = 0.3$ and $z = 0.7$.

4.2. *Contamination from field galaxies and galactic stars*

Because of our ability to identify the cluster members, we avoid the uncertainties inherent to statistical methods of removing the field contamination. As a check of the reliability of this approach to estimate redshift and morphological type also for non-cluster galaxies, we now compare the field contamination we found directly in the Cl 0016 + 161 field with the values expected from Tyson (1988).

In the redshift window we analyzed ($0.3 \leq z \leq 0.7$) and with the membership criterion we adopted (Sect. 4.1), we found 48 foreground and background galaxies. According to Tyson we should find 58 field galaxies with $R \leq 22.5$ in a $3.5' \times 5'$ field. The first obvious explanation of this discrepancy is that some of them have certainly redshifts outside the interval taken in consideration. Furthermore, because the filters are optimized to detect cluster galaxies,

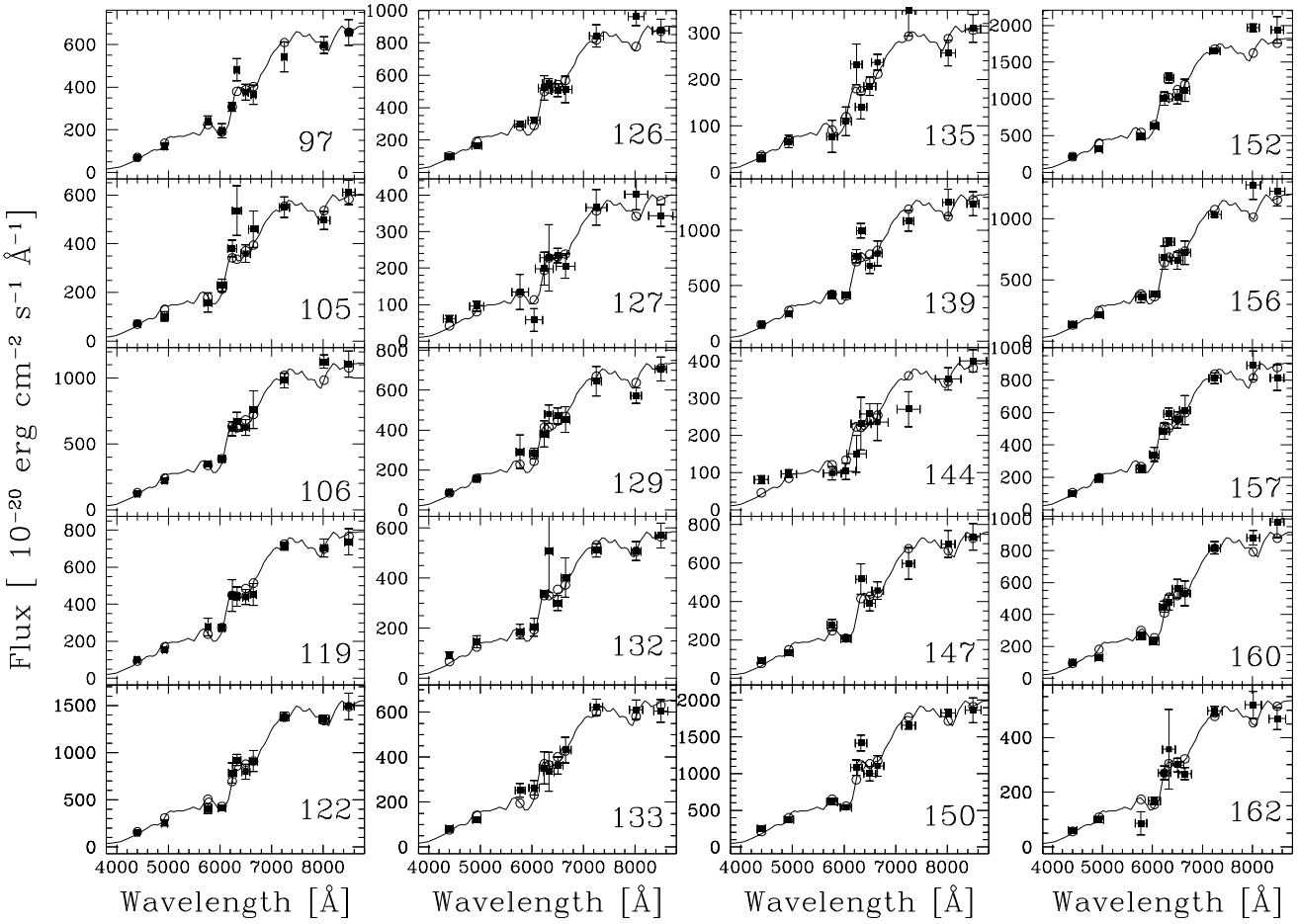

Fig. 9. Examples of low-resolution spectra of elliptical galaxies in Cl 0016 + 161. Same simbols as in Fig. 7. The galaxies 139, 150, 152, 156 and 160 are already known to be members from Dressler & Gunn (1992)

even some of the field galaxies inside the redshift window analyzed could belong to the 39 not classified objects because no dominant features can be easily recognized with the filter setup used.

We also made an estimation of the contamination from stars in the field. In spite of using the objects' point spread function as a criterion to disentangle stars from galaxies we tried to fit the observed fluxes with additional SED templates for stellar types (Belloni et al. 1995). Because the most serious contamination in the 19-23 magnitude range is caused by M dwarfs (Mihalas & Binney 1981), we restricted ourselves to templates of M-type stars' SED. Obviously, very bright objects were also straightforward recognized as stars. The discrepancy between our results (12 stars in the field) and the extrapolated counts for all types of stars brighter than $R = 22.5$ mag in this area of the sky (20 stars, Bahcall & Soneira 1981a, b), can be due to the neglect of other stellar types. Moreover, some of the missed stars may belong to the 39 non-classified objects.

5. Conclusion

We systematically analyzed all objects brighter than $R = 22.5$ magnitude and within about 1.5 Mpc of the center of clusters $0939 + 472$ and $0016 + 161$. This provided us with a sample of more than one hundred galaxy cluster members representing a significant improvement over the most complete study to date (DG92). Indeed, although these two clusters may be considered among the best studied, only about 30 spectra per cluster are available, so that any conclusion reached to date about their galaxy populations relies on these few spectra.

In particular, the big sample of ellipticals obtained is well suited for a study of evolutionary effects in the early-type galaxy population that will be the subject of a forthcoming paper. For this purpose beside the importance of a secure membership two other aspects of our approach are of great relevance. First, with the selection criterion we applied to define the elliptical sample we are able to recognize galaxies with a SED matching that of an elliptical

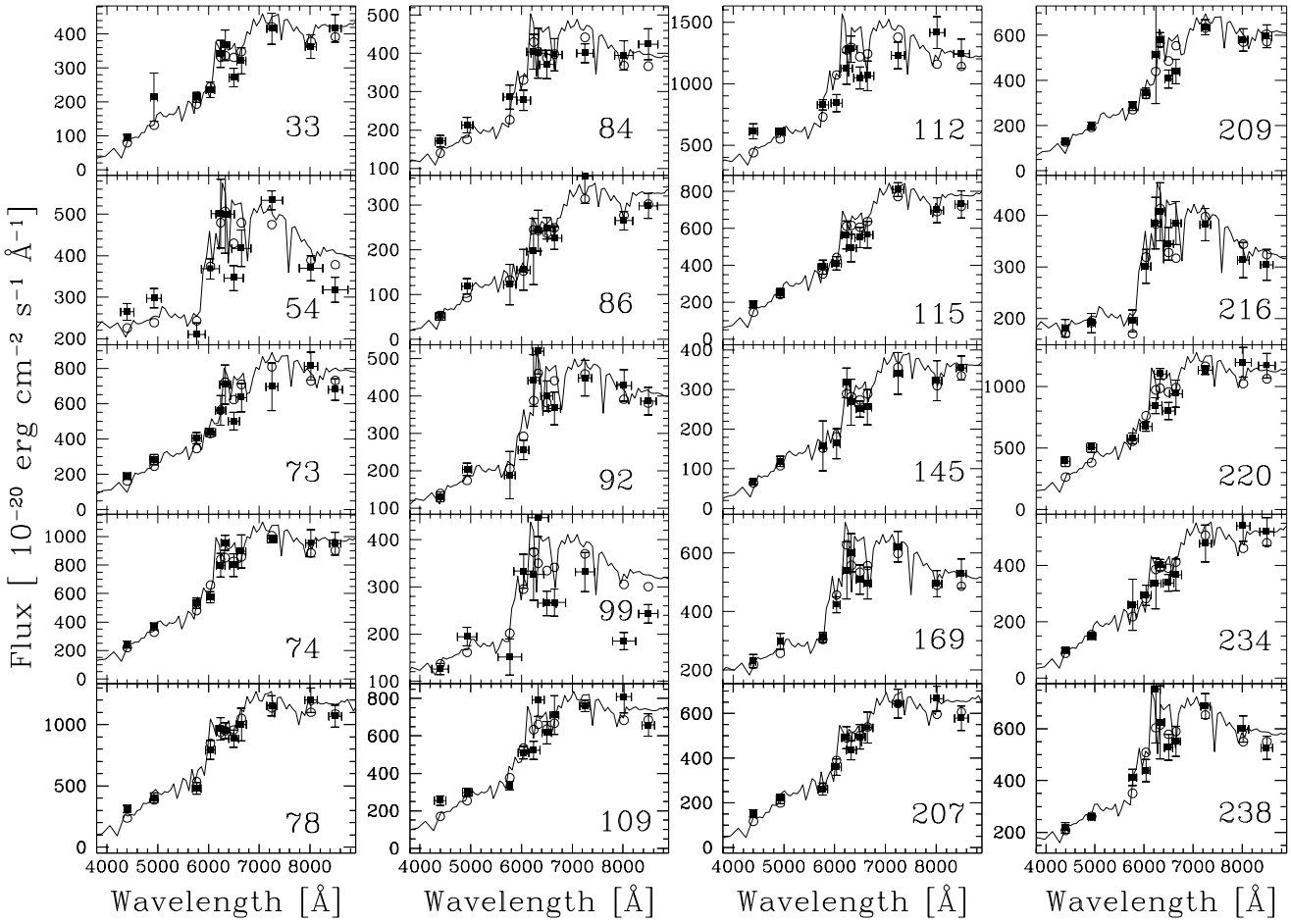

Fig. 10. Low-resolution spectra of all E+A galaxies in Cl 0016 + 161. Same simbols as in Fig. 7. The galaxies 54, 73, 78, 84, 99, 109, 112, 207, 220 and 238 are already known to be members from Dressler & Gunn (1992)

over a wide wavelength range but with an excess of blue flux. Second, the cutoff of our galaxy sample has been set 3 magnitudes fainter than the present-day L^* allowing us to cover a significant tail of the cluster luminosity function and then bring into view secondary episodes of star formation in low luminosity ellipticals (Rose 1984; Faber et al. 1995).

This last point has been addressed in detail in our work through the analysis of E+A galaxies. To identify these galaxies in Cl 0016 + 161 in a reliable and efficient way we applied the same templates developed for Cl 0939 + 472 in Belloni et al. (1995). About all of the already known E+A galaxies have been correctly identified and new ones discovered. The only two discordant cases have a SED significantly different from that of the typical E+A galaxies found in the literature. Moreover, a preliminary follow up spectroscopy of some of the new candidates confirmed the reliability of our method in recognizing this non standard SED.

In summary, we found that in both clusters E+A galaxies represent about 20% of the total galaxy population. This outlines the importance of taking into account features of previous phases of star formation in galaxies in high redshift clusters to correctly quantify the Butcher-Oemler effect. We note that the analysis of E+A galaxies presented here has been carried out under the assumption that they result from a recent burst of star formation in an elliptical galaxy. It is possible instead that the starburst takes place in spiral galaxies through their interactions with other cluster members or with the intercluster medium (Moore et al. 1996; Bothun & Gunn 1986). HST images, indeed, show that the morphology of this population is controversial. They have appeared bulge-like in AC114 (Couch et al. 1994) and disk-like or irregular in Cl 0939 + 472 and Cl 0016 + 161 (Dressler et al. 1994; Wirth et al. 1994).

As already noticed (Charlot & Silk 1994; Belloni 1994) it is the sudden switching on of a higher star formation

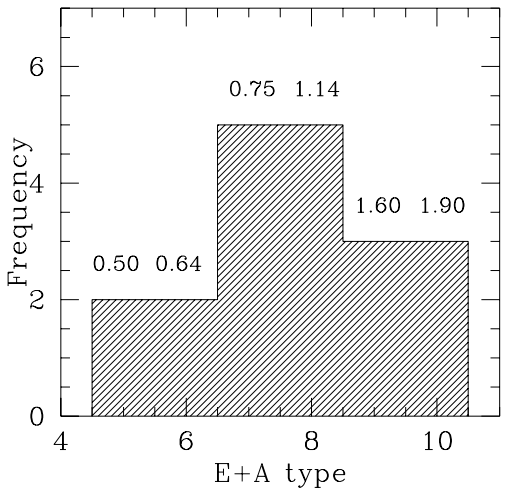

Fig. 11. Histogram of the age distribution of the 20 E+A cluster members. E+A types from 5 to 10 represent galaxies seen from 0.5 to 1.90 Gyr after the beginning of the second burst

rate that is crucial to the production of E+A spectra, not the morphological type of the underlying galaxy hosting the burst. In Paper II we will analyze in detail the E+A SEDs predicted by the new Bruzual & Charlot (1996) population synthesis models in the case of an underlying spiral galaxy. Here we only emphasize that the E+A templates so obtained cannot be disentangled from those considered in this paper, at least with the spectral resolution allowed by narrow band photometry. This signifies that our approach in identifying E+A galaxies is independent of the assumption made about their formation mechanism and strongly confirms the robustness of our results.

Acknowledgements. We are very much in debt to the Calar Alto staff for the constant support during the observations. We would like to thank G. Bruzual for having made his programs available and for his interest in this project.

References

Aragon-Salamanca A., Ellis R.S., Couch W.J., Carter D., 1993, MNRAS 262, 764
Bahcall J., Soneira R., 1981a, ApJS 47, 357
Bahcall J., Soneira R., 1981b, ApJ 246, 122
Belloni P., Bruzual G.A., Thimm G.J., Röser H.-J., 1995, A&A 297, 61
Belloni P., 1994, Ph.D. thesis, University of Heidelberg
Belloni P, Röser H.-J., 1996, A&A (in preparation)
Bower R.C., Lucey J.R., Ellis R.S., 1992, MNRAS 254, 601
Bruzual G., 1983, ApJ 273, 105
Bruzual G., Charlot S., 1993, ApJ 405, 538
Bruzual G., Charlot S., 1996, ApJ (in preparation)
Burstein D., Heiles C, 1982, AJ 87, 1165
Butcher H., Oemler A., 1978, ApJ 219, 18
Charlot S., Silk J., 1994, ApJ 432, 464
Coleman G.D., Wu C.C., Weedman D.W., 1980, ApJS 43, 393
Couch W.J., Sharples R.M., 1987, MNRAS 229, 423
Couch W.J., Ellis R., Sharples R., Smail I., 1994, ApJ 430, 121
Dickinson M., 1995, in ASP Conf. Ser., Fresh view of Elliptical Galaxies, Buzzoni A. et al. (eds.), p. 283
Dressler A., 1980, ApJ 236, 351
Dressler A., Gunn J., 1983, ApJ 270, 7
Dressler A., Gunn J.R.E., 1992, ApJS 78, 1 (DG92)
Dressler A., Schectman A., 1987, AJ 94, 899
Dressler A., Oemler A., Butcher H.R., Gunn J.R.E., 1994, ApJ 430, 107
Ellis R.S., Couch W.J., MacLaren I., Koo D.C., 1985, MNRAS 217, 239
Gunn J.E., Hoessel J.G., Oke J.B., 1986, ApJ 306, 30
Faber S.M., Trager S.C., Gonzalez J.J., Worthey G., 1995, in IAU Symp. 164, Van der Kruit P.C. & Gilmore G. (eds.). Kluwer, Dordrecht, p. 249
Henry J.P., Gioia I.M., Maccacaro T., Morris S.L., Stocke J.T., Wolter A., 1992, ApJ 386, 408
Koo D.C., 1981, ApJ 251, L75
Lavery R., Henry J., 1986, ApJ 304, L5
Lavery R., Henry J., ApJ 323, 473
Massey P., Gronwall C. 1990, ApJ 358, 344
Mihalas D., Binney J.J., 1981, Galactic astronomy, 2nd ed. San Francisco, Ed. Freeman
Moore B., Katz N., Lake G., 1996, in IAU Symp. 171, Bender R. and Davies R. (eds.). Kluwer, p. 203
Pickles A.J., 1985, ApJ 296, 340
Pickles, Van der Kruit, 1991, A&AS 91, 1
Rose J.A., 1984, AJ 89, 1238
Rose J.A., 1985, AJ 90, 1927
Röser H.-J., Meisenheimer KI., 1991, A&A 252, 458
Thimm G.J., Röser H.-J., Hippelein H., Meisenheimer K., 1994, A&A 285, 785
Tyson J.A., 1988, AJ 96, 1
Wirth G.D., Koo D.C., Kron R.G., 1994, ApJ 435, L105
Wirth G.D., Belloni P., 1996, ApJ (submitted)
Visvanathan S., Sandage A., 1977, ApJ 216, 214

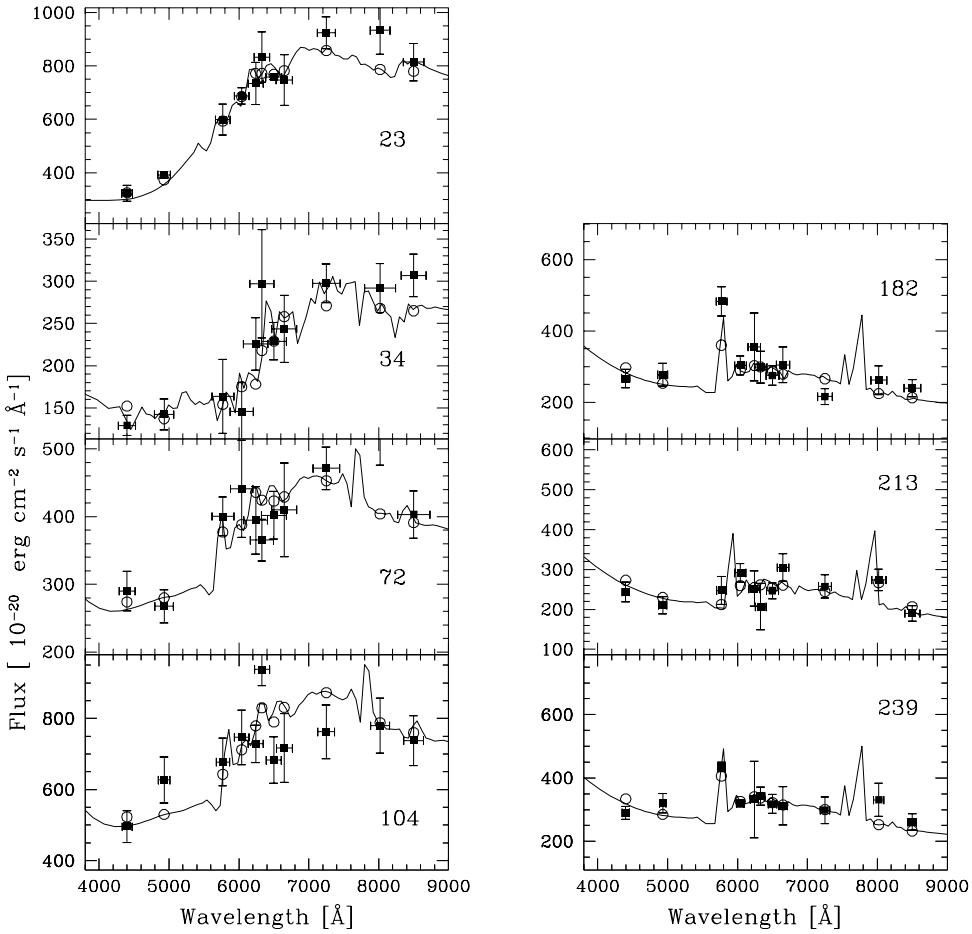

Fig. 12. Low-resolution spectra of all galaxies classified as spiral or irregular in Cl 0016 + 161. Same simbols as in Fig. 7. The galaxies 213 and 239 are the only emission lines members already known from Dressler & Gunn (1992)

Table 4. Results of the analysis of the 323 objects brighter than $R = 22.50$ mag. in the Cl 0939 + 472 field. x and y are the coordinates as in DG92, $Z_{\rm D}$ indicates the redshift from DG92, z is that obtained in this work with 1 σ_z deviation

N$_{\rm o}$	x [$''$]	y [$''$]	R	$B-R$	$B-I$	$\tilde{D}_{4000}$	$Z_{\rm D}$	z	σ_z	Type
1	-55.73	92.87	22.4	1.3	2.1	1.9		0.54	0.03	Scd
4	-58.79	91.83	22.5	2.0	3.1	2.4		?	?	
5	-86.30	91.96	21.3	1.1	1.8	1.5		0.52	0.01	Im
8	36.94	90.78	21.7	2.5	3.7	1.6		0.42	0.04	E
9	-108.22	90.18	16.2	0.5	1.5	1.4		star		
14	-124.85	89.08	22.1	1.7	2.5	1.5		0.42	0.03	Scd
17	-72.54	87.99	21.9	1.4	2.3	1.5		0.41	0.03	Scd
22	-184.11	85.63	21.9	1.9	3.2	2.2		0.41	0.05	E
25	38.70	84.37	20.7	2.6	3.8	2.2		?	?	
26	-44.05	84.33	22.4	1.1	1.8	1.2		0.52	0.03	Im
27	-179.07	84.47	22.4	2.1	3.1	2.0		0.50	0.06	Sbc
30	-13.85	82.70	21.6	1.7	2.7	1.1		?	?	
32	58.44	81.21	22.0	2.6	4.1	1.0		?	?	
36	-113.61	80.34	20.6	1.4	2.3	2.0		0.40	0.01	Sbc
37	42.00	79.54	22.5	2.2	3.3	1.4		?	?	
38	-73.29	79.70	22.2	1.4	2.4	1.4		0.39	0.02	E+A
39	-55.16	78.36	19.8	1.6	2.5	1.4		0.44	0.03	Sbc
40	11.53	77.34	22.0	2.1	3.2	1.4		0.66	0.05	Sbc
41	-20.02	76.85	18.5	1.8	2.9	1.4		?	?	
44	-33.52	74.58	22.0	1.2	1.8	1.3		0.52	0.01	Im
45	-92.55	74.98	21.8	2.0	3.0	1.8		0.42	0.03	E+A
47	-47.74	74.23	20.9	2.4	3.6	2.6		0.41	0.02	E
48	-68.69	74.30	22.3	2.4	3.6	2.4		0.42	0.02	E
49	-153.10	74.18	22.2	1.5	2.2	1.3		0.55	0.03	Scd
50	20.97	73.18	22.0	1.1	1.6	1.0		0.41	0.02	Im
51	-74.66	73.17	22.0	2.1	3.1	1.9		0.43	0.04	E+A
61	49.44	71.35	21.4	2.4	3.7	1.8		0.44	0.04	E
62	4.01	71.21	21.3	2.4	3.7	2.3		0.42	0.02	E
63	-71.35	71.43	20.7	2.0	3.0	1.7		0.40	0.02	E+A
64	-155.73	70.94	22.3	1.5	2.4	1.6		0.43	0.03	Sbc
65	-200.93	71.60	20.8	2.6	3.9	3.9		?	?	
69	49.43	69.72	22.5	1.3	2.3	1.0		?	?	
74	-141.42	68.04	21.0	2.4	3.6	2.6		0.42	0.02	E
75	-37.13	67.60	20.0	2.0	3.1	1.7		0.42	0.02	E+A
81	-20.24	65.42	21.9	2.1	3.3	2.1		0.42	0.03	E
82	39.11	64.69	21.3	1.4	2.2	1.3		?	?	
84	57.05	63.46	22.0	1.4	1.9	1.0		0.58	0.06	Im
88	-1.86	60.94	21.4	2.2	3.4	1.9	0.4080	0.43	0.02	E
89	-24.80	61.21	22.1	1.9	2.9	1.7		0.41	0.02	E+A
90	-66.92	61.23	22.4	2.3	3.3	2.2		0.41	0.02	E
91	-144.84	61.32	20.8	2.2	3.3	1.8		0.41	0.01	E+A
97	-7.79	56.56	20.6	2.4	3.6	2.3	0.4027	0.42	0.02	E
98	-44.43	56.55	22.4	1.9	2.9	2.6		0.41	0.01	E
99	49.67	56.12	22.4	1.1	1.7	1.0		0.58	0.04	Im
104	-191.18	55.09	22.2	2.5	3.6	2.9		0.41	0.04	E
107	-56.91	53.76	21.9	1.8	2.8	1.8		0.42	0.03	E+A